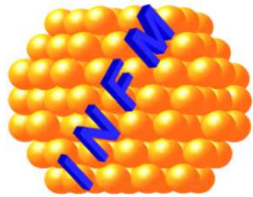


Electron Spin Resonance (ESR) investigation of paramagnetic point defects in ^{17}O doped Si-FZ irradiated with 27MeV electrons

**Sergiu V. NISTOR, Daniela GHICA, Alexandra C. JOITA,
Roxana RADU and Ioana PINTILIE**



***National Institute of Materials Physics
Magurele, Romania***



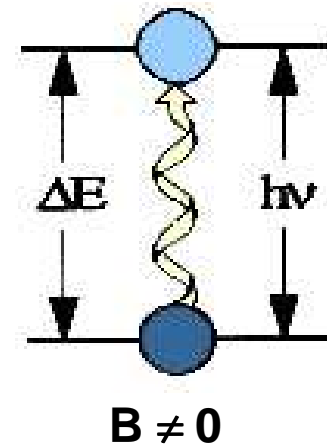
Presented at the RD50 workshop, Bucharest, June 11-13, 2014

Content

- I. ESR in determining the presence and structure of lattice defects.
- II. ESR of irradiation paramagnetic point defects (IPPDs) in Si for radiation detectors.
 - A. Objectives and workplan.
 - B. Experimental conditions. Samples and instruments.
- III. Preliminary results on e⁻(27MeV) irradiated:
 - A. Si-FZ doped by diffusion with ¹⁷O enriched isotope.
 - B. Si-FZ implanted with ¹³C enriched isotope (low oxygen content).
- IV. Synthesis of results. Analysis of available data.
- V. Conclusions.

I. Electron Spin Resonance (ESR) in determining the presence and structure of lattice defects.

- ❑ **The best technique-method to determine the structure of point defects in semiconductors (Si, diam., GaAs, ZnS, ...)**
- ❑ **ESR = Zeeman ($B \neq 0$) spectroscopy of defects with $S \neq 0$ ($S = 1/2, 1, \dots$) electron states.**
- ❑ **The condition of resonance: $\Delta E = h\nu$**
- ❑ **$\nu \rightarrow 9.5 - 34 \text{ GHz}, \dots, 250 \text{ GHz}$**



Electrons in the magnetic field. The electron Zeeman interaction.

Electrons angular momentum →

magnetic moment → spin states

- Orbital motion: $\mu_L \rightarrow \mu_B L$;

- Intrinsic or “spin”: $\mu_S \rightarrow -g_e \mu_B S$

$$g_e = 2.00232,$$

$$\mu_B = eh/2m_e = 9.274 \times 10^{-24} \text{ J / T}$$

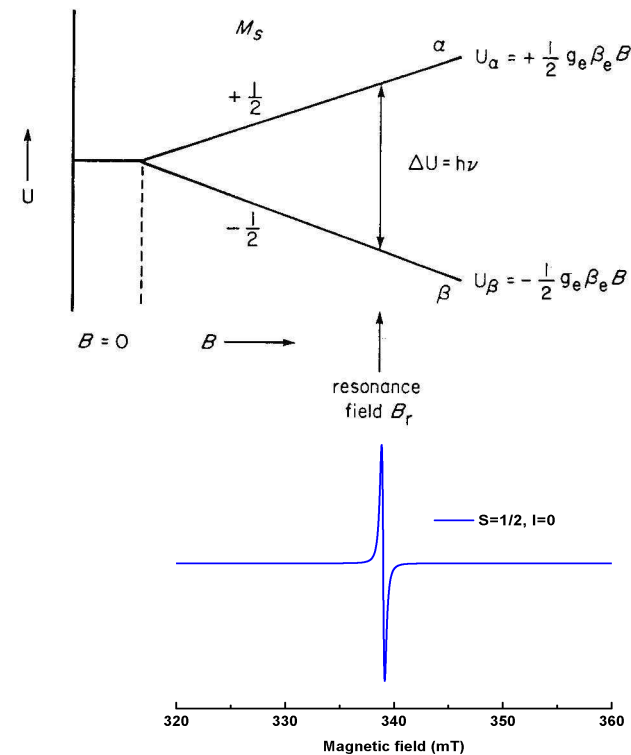
The electronic Zeeman interaction

$$H_Z = -\mu_S \cdot B = g_e \mu_B S \cdot B$$

For $S = 1/2$ ($M_S = \pm 1/2$) →

$$\rightarrow U_Z(M_S) = g_e \mu_B B M_S = \pm g_e \mu_B B$$

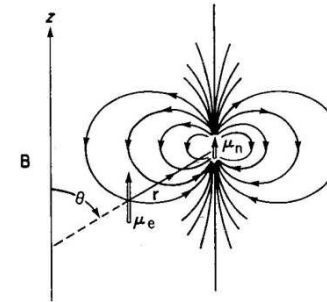
$$\rightarrow h\nu = g_e \mu_B B \rightarrow B = h\nu / g_e \mu_B$$



S = 1/2 system in a magnetic field

Hyperfine interactions

The unpaired electron spin (S) of the defect interacts with the nuclear spins (I_i) of the defect atoms: $H_{hf} = \sum_i (S \cdot A \cdot I_i - g_n \mu_n I_i \cdot B)$



The isotropic case

for $S = I = 1/2$, $A > 0$

$$H = g\mu_B \mathbf{S} \cdot \mathbf{B} + A \mathbf{S} \cdot \mathbf{I}$$

$$U(M_S, M_I) = g\mu_B B M_S + A M_S M_I$$

Two allowed transitions:

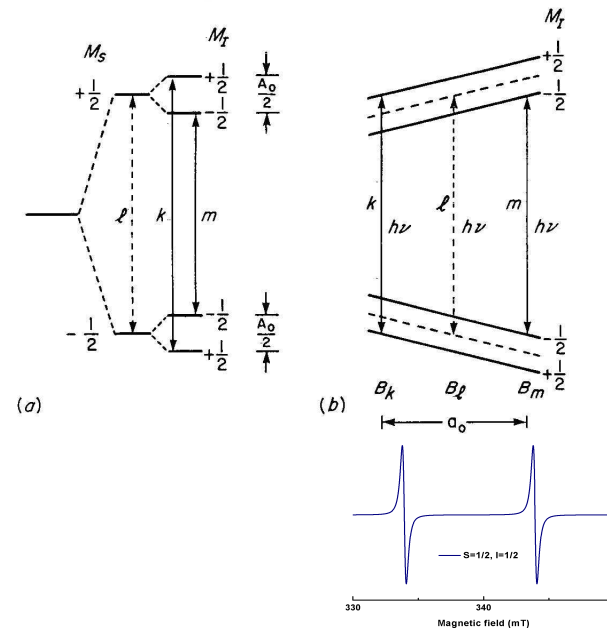
$$(U_{Zeeman} > U_{hf}; \Delta M_S = \pm 1, \Delta M_I = 0)$$

$$h\nu_{k,m} = g\mu_B B \pm \frac{1}{2}A$$

Transition fields:

$$B_k = h\nu/g\mu_B - A/2g\mu_B \quad (M_I = +1/2)$$

$$B_m = h\nu/g\mu_B + A/2g\mu_B \quad (M_I = -1/2)$$



$S = 1/2, I = 1/2$ system in a magnetic field

The anisotropic spin Hamiltonian ($S=1/2$)

$\mu_L \neq 0$!! \rightarrow SO + CF interactions

$$H_{SH} = \mu_B \mathbf{S} \cdot \mathbf{g} \cdot \mathbf{B} + \mathbf{S} \cdot \mathbf{A} \cdot \mathbf{I}$$

Particular cases (local symmetry) ($S = 1/2, I \neq 0$):

Rhombic: $H_{SH} = \mu_B [g_x B_x S_x + g_y B_y S_y + g_z B_z S_z] + A_x S_x I_x + A_y S_y I_y + A_z S_z I_z$

Axial: $H_{SH} = g_{\perp} \mu_B (B_x S_x + B_y S_y) + g_{\parallel} \mu_B B_z S_z + A_{\perp} (S_x I_x + S_y I_y) + A_{\parallel} S_z I_z$

Cubic: $H_{SH} = g \mu_B (B_x S_x + B_y S_y + B_z S_z) + A (S_x I_x + S_y I_y + S_z I_z)$

The g-anisotropy general case

$$\mathbf{B} = (l, m, n) B$$

$$U = \mu_B (g_x^2 l^2 + g_y^2 m^2 + g_z^2 n^2)^{1/2} B m_s = \mu_B g B m_s$$

g-value depends on B direction !

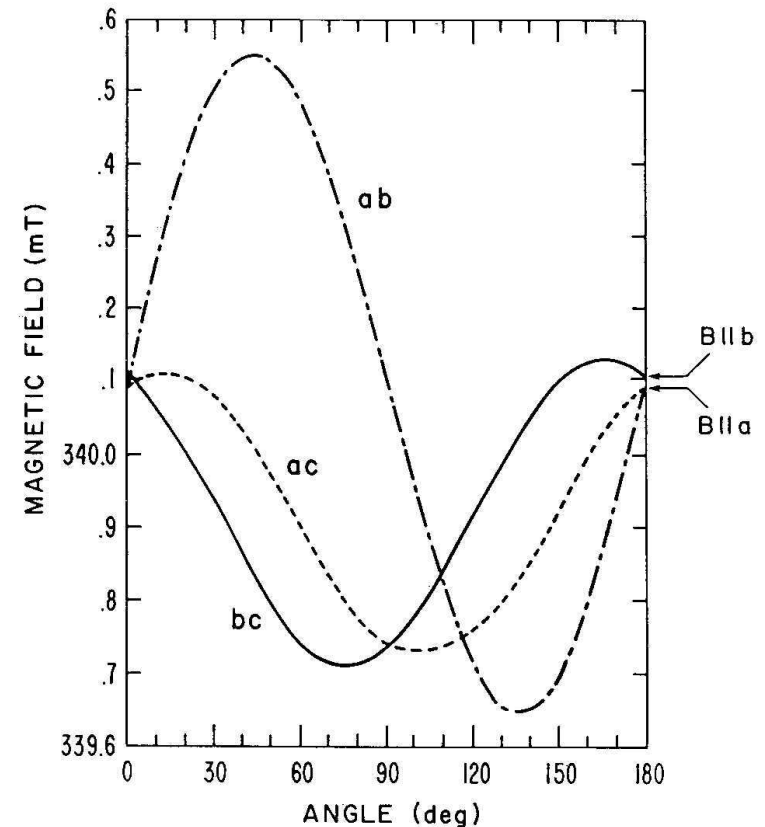
Rhombic: $g^2 = g_x^2 l^2 + g_y^2 m^2 + g_z^2 n^2$

Axial: $g^2 = g_{//}^2 \cos^2 \theta + g_{\perp}^2 \sin^2 \theta$

g_x, g_y, g_z principal values along x, y and z directions

$$g^2 = (gg)_{xx} \sin^2 \theta \cos^2 \varphi + 2(gg)_{xy} \sin^2 \theta \cos \varphi \sin \varphi + (gg)_{yy} \sin^2 \theta \sin^2 \varphi + 2(gg)_{xz} \sin \theta \cos \theta \cos \varphi + 2(gg)_{yz} \sin \theta \cos \theta \sin \varphi + (gg)_{zz} \cos^2 \theta$$

(ab): $\theta = 90^\circ$; (bc): $\varphi = 90^\circ$; (ca): $\varphi = 0^\circ$



g-variation in the main crystal planes

Investigating defects in semiconductors by ESR

- ❑ ESR spectra observation \Rightarrow presence and concentration of paramagnetic defects \Rightarrow Sensitive: 2×10^{10} spins/Gauss (~ 1 ppb)
- ❑ High resolution \Rightarrow separation of the overlapping spectra from different centers. Linewidth vs. T and I vs. μ W power are used to identify the spectra lines of different centers.
- ❑ Spectra anisotropy \Rightarrow *reflects local structure !*
- ❑ Hyperfine structure \Rightarrow atomic structure (ENDOR).
- ❑ Spin Hamiltonian (SH) parameters \Rightarrow information on ground state quantum properties. Each center is fully characterized by its SH !
- ❑ The resulting info. \Rightarrow Defect atomic structure.

II. Electron Spin/Paramagnetic Resonance investigation of irradiation paramagnetic point defects (IPPDs) in Si for radiation detectors.

Main objective:

- **To determine in the crystalline Si used in the tracking detectors at LHC from CERN the presence and structure of the IPPDs suggested to be involved in their radiation induced performance degradation.**

How

- **Observing and characterizing by ESR the IPPDs.**
- **Correlating the ESR findings with the TSC results.**

II. ESR investigations of IPPDs in Si for radiation detectors. *The workplan.*

- Observing and recording the EPR spectra in the as-irradiated and post-annealed samples, at $296\text{ K} > T > 10\text{ K}$, with B in (110), for low / high μW powers, with across the gap illumination too.
- Determine the spectra of different IPPDs from the specific I vs. T, I vs. μW power and angular dependence behavior.
- Determine the local symmetry and SH parameters with ESR lines simulation and fitting software \Rightarrow **Structure of the IPPDs.**
- Correlate the ESR and TSC data. Comparing the production properties vs. isochronal T_{ann} of the observed defects.

Determining the structure of the lattice point defects in Si from ESR

- ESR resulted in the observation and characterization of several hundredths of irradiation paramagnetic point defects (IPPDs) in Si. **The best investigated semiconductor!**
- Tables of characteristic (spin Hamiltonian) parameters (see Landolt-Boernstein, vol. III/22b-41A.2a), **as reference for the known IPPSs !**
- Accurate determination of a defect structure requests, besides the symmetry and SH parameter values, mapping of hyperfine interactions with nuclei of the involved atoms (ESR/ENDOR).
- For silicon with ^{29}Si ($I=1/2$) isotope of 4.685% nat. abundance, one needs high intensity spectra ($s/n > 50$).
- ^{17}O ($I=5/2$; 0.038%) and ^{13}C ($I=1/2$; 1.07%) request doping with enriched isotopes.

IIB. Experimental conditions: the instruments

Q-band ESR spectrometer ELEXSYS 500Q with optical cryostat and probe head for 300K to 3.8 K measurements and goniometer for monitoring sample rotation. ⇒

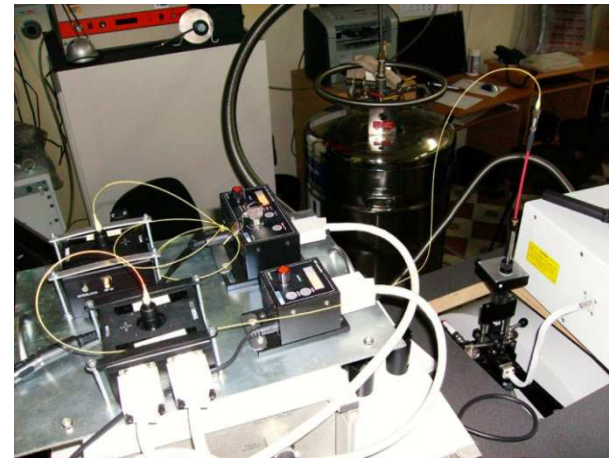
Sensitivity: 2×10^{10} spins/Gauss

Maximum magnetic field: 1.8 T.

Stability/accuracy: better than 10^{-6} .

In-situ optical excitation:

- Frontal window (UV, laser beams)
 - From above, with the optical fiber through the sample holder, using a laser diode (637nm, 70 mW max. output) as light source.
- ⇒



II.B. Experimental conditions: the investigated samples

ESR samples were cut from two types of Si-FZ100 platelets (Wacker, n-type, 5 kOhm.cm) of $5 \times 5 \times 0.3 \text{ mm}^3$ size, irradiated with 27MeV electrons (dose = 2.00×10^{16}), as follows :

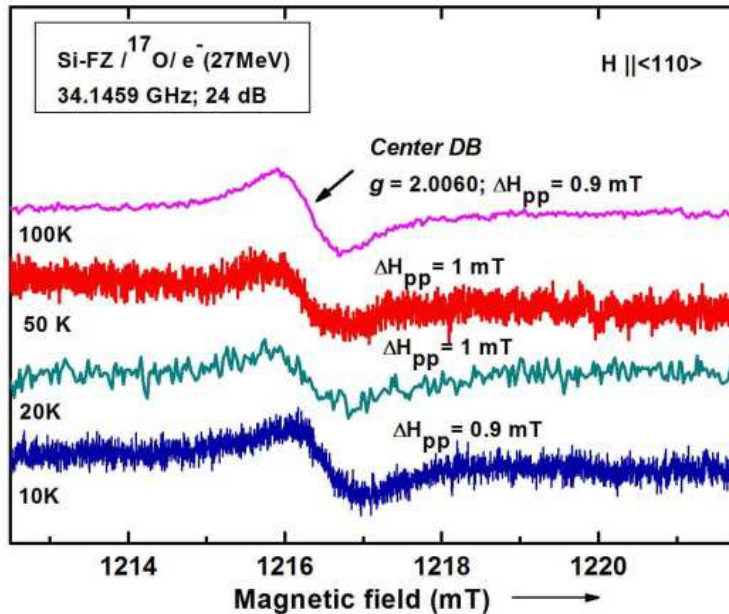
- **Si-FZ100-17O (70% ^{17}O doped by diffusion, conc. = 1.2×10^{17} – from SIMS)**
- **Si-FZ100-13C (3MeV implanted; dose 5×10^{13} ; ^{16}O conc. = 1×10^{16} - STFZ)**

The ESR samples, of $0.3 \times 0.18 \times 4 \text{ mm}^3 = 2.16 \text{ mm}^3$, were cut with the long axis $\parallel \langle 110 \rangle$.

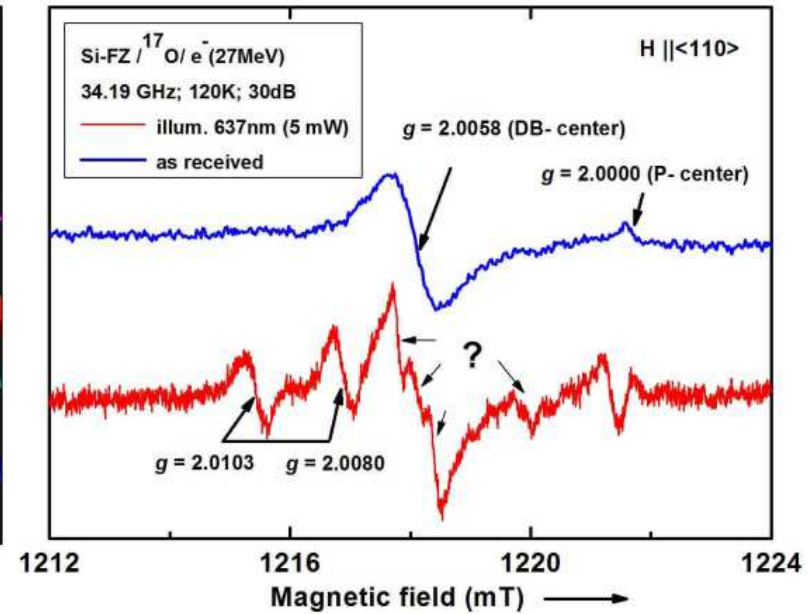
- **Samples in ESR holder with rotation axis $\parallel \langle 110 \rangle \Rightarrow \mathbf{B}$ in (110)**
- **Estimated defects sensitivity threshold in the sample: $\sim 5 \times 10^{12}$**
- **Impurity conc. in ESR samples: $^{17}\text{O} = 2.4 \times 10^{14}$ (DOFZ); $^{16}\text{O} = 2 \times 10^{13}$ (STFZ)**

IIIA. Experimental results on e^- (27MeV) irradiated Si-FZ-170 samples.

ESR spectra vs. T_{meas} and 637nm optical in-situ excitation



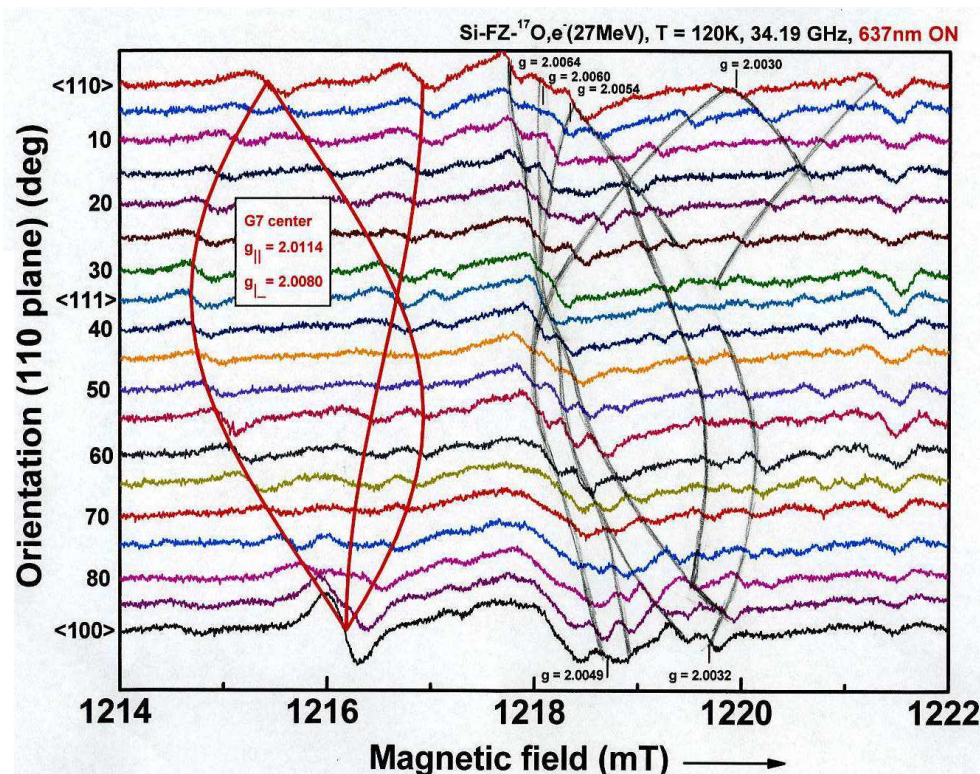
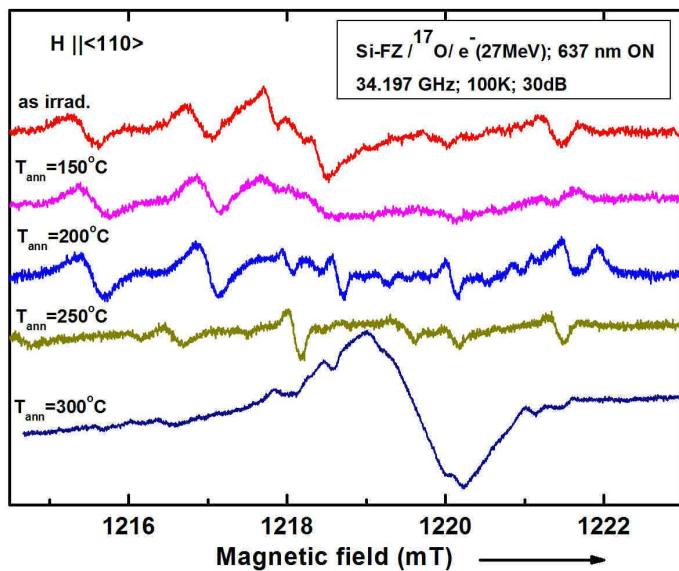
ESR spectrum of the isotropic DB center



The observed photoinduced (637nm) ESR signals, are stable at $T < 150\text{K}$.

III.A. Experimental results on e^- (27MeV) irradiated Si-FZ-170 samples.

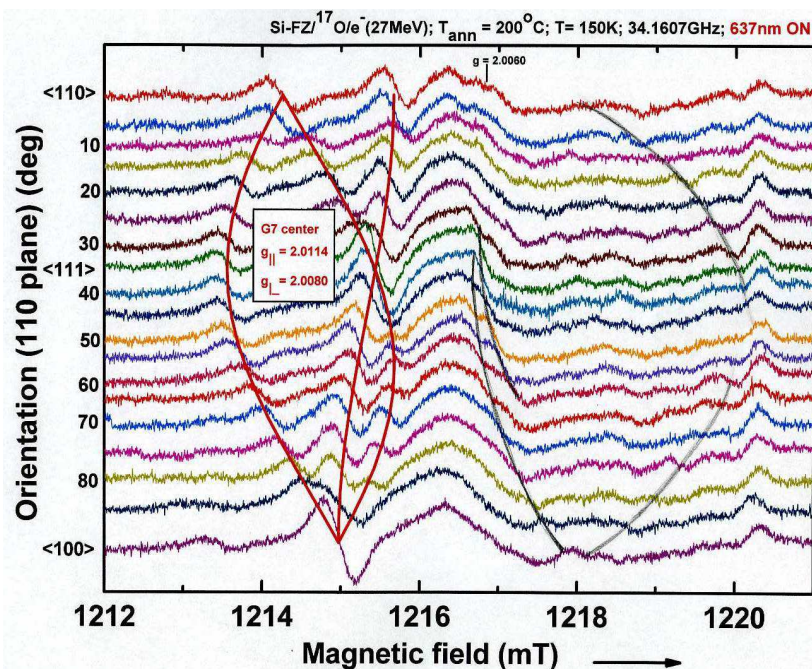
Thermal annealing produces changes in the photo induced ESR spectra/centers.



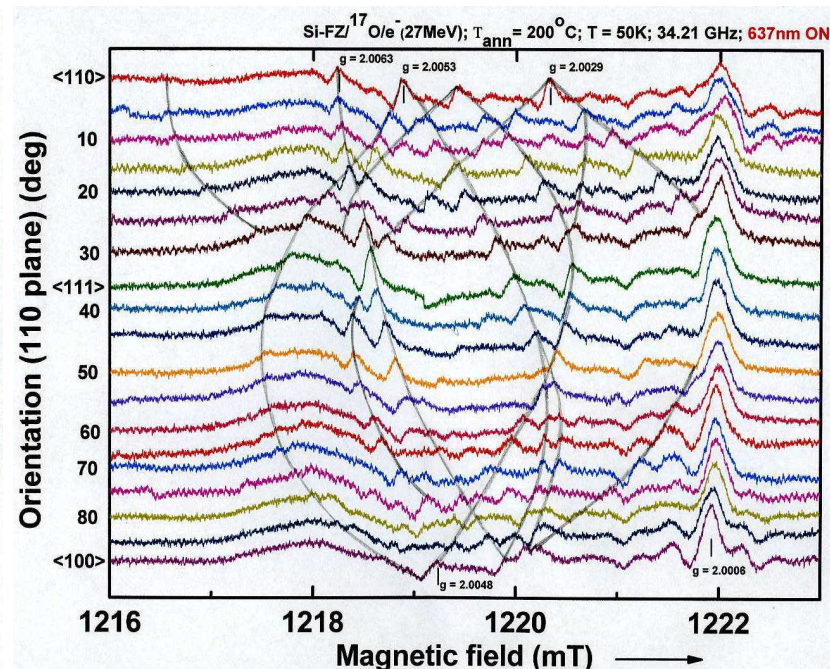
IPPDs in the as-irradiated sample. Identified center (G7) – red lines. Unidentified centers – black lines.

IIIA. Experimental results on $e^-(27\text{MeV})$ irradiated Si-FZ-170 samples.

Photoinduced ESR spectra in annealed samples. The $T_{\text{meas.}}$ effects.



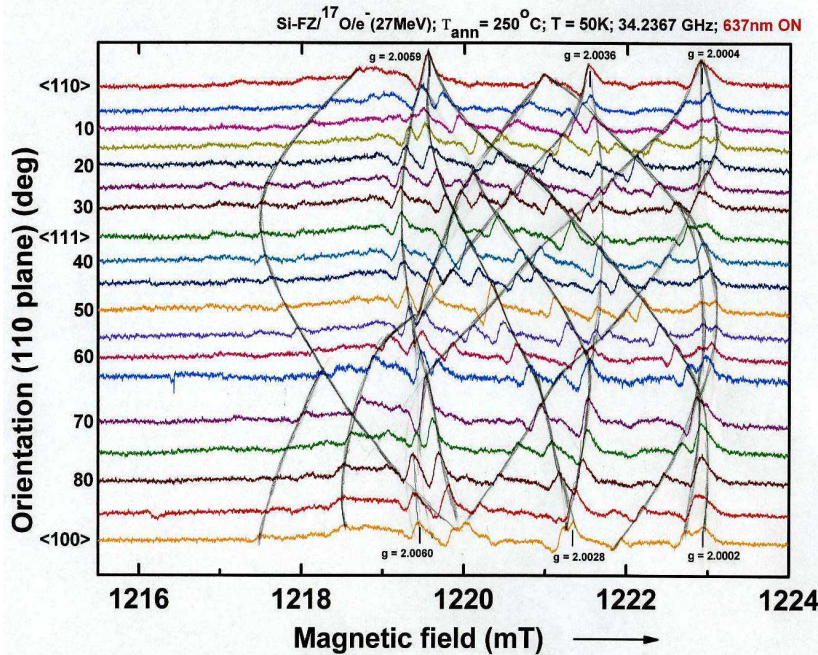
$T_{\text{ann}}=200^\circ\text{C}$; $T_{\text{meas}}= 150\text{K}$
 Absorption mode.



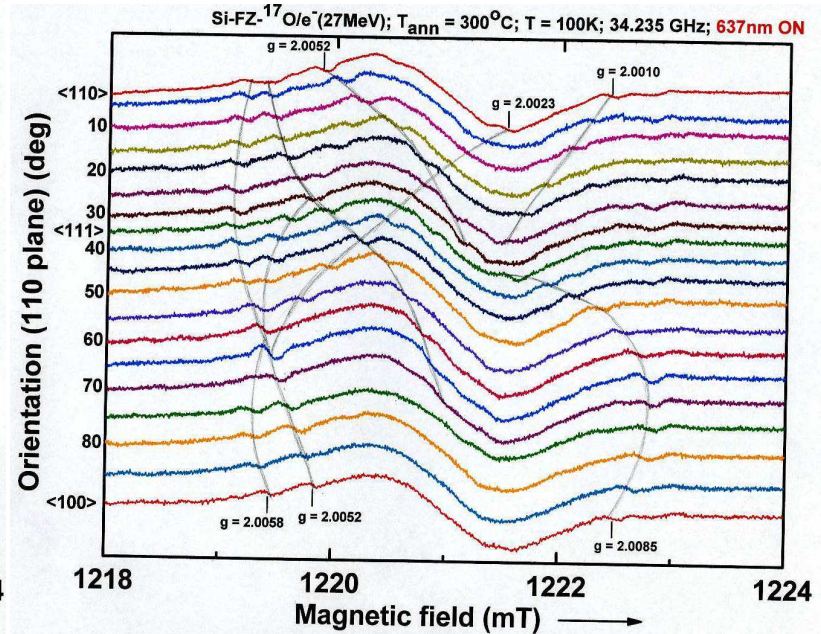
$T_{\text{ann}}=200^\circ\text{C}$; $T_{\text{meas}}= 50\text{K}$
 Dispersive mode. Increased sensitivity !

III.A. Experimental results on $e^-(27\text{MeV})$ irradiated Si-FZ-170 samples.

New paramagnetic centers produced by annealing.



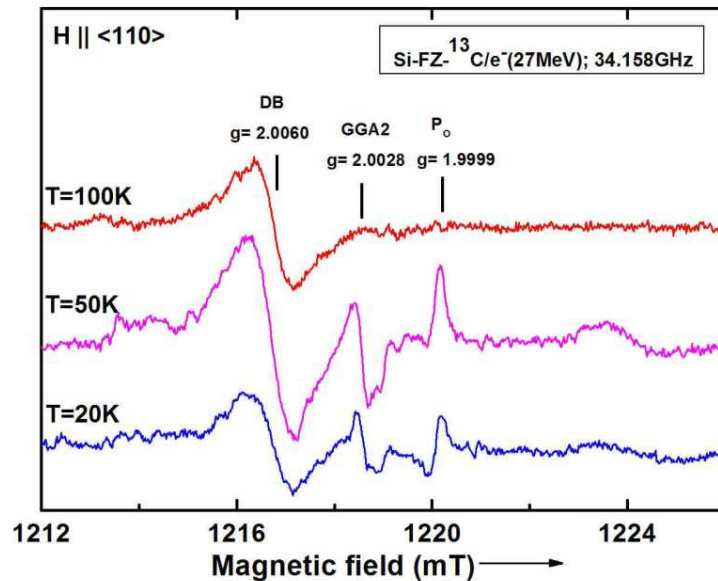
$T_{\text{ann}} = 250^\circ\text{C}$; $T_{\text{meas}} = 50\text{K}$
Dispersive mode.



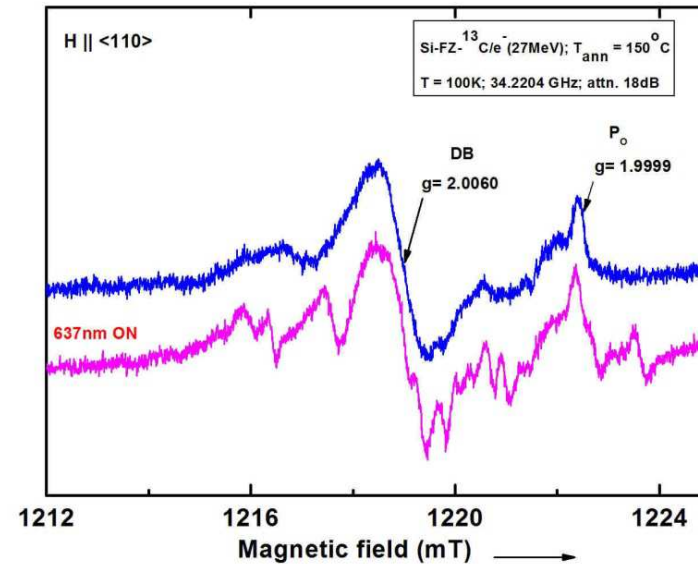
$T_{\text{ann}} = 300^\circ\text{C}$; $T_{\text{meas}} = 100\text{K}$
Absorption mode.

IIIB. Experimental results on $e^-(27\text{MeV})$ irradiated Si-FZ-13C samples.

ESR spectra vs. T_{meas} and 637nm optical in-situ excitation



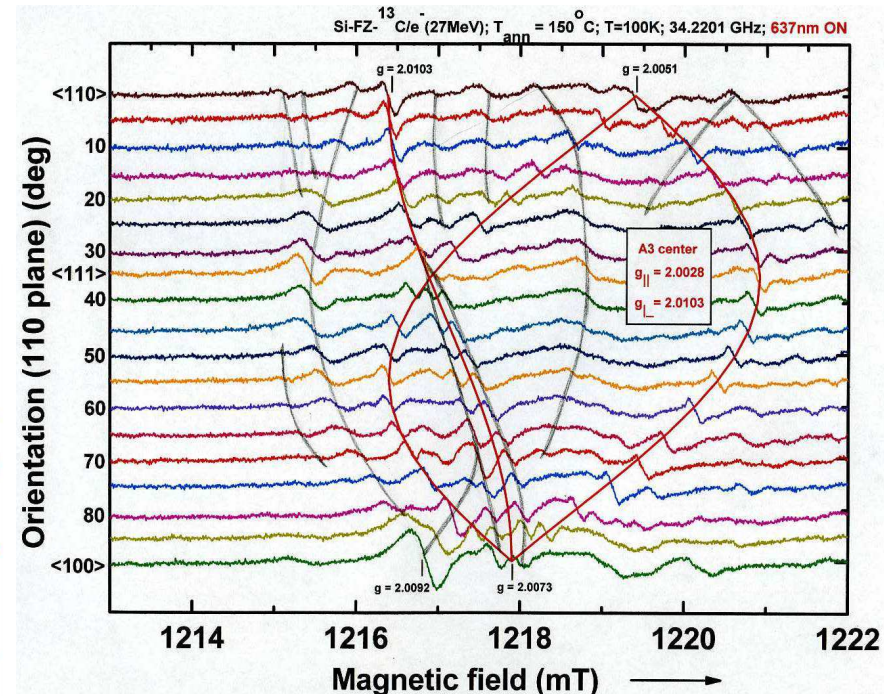
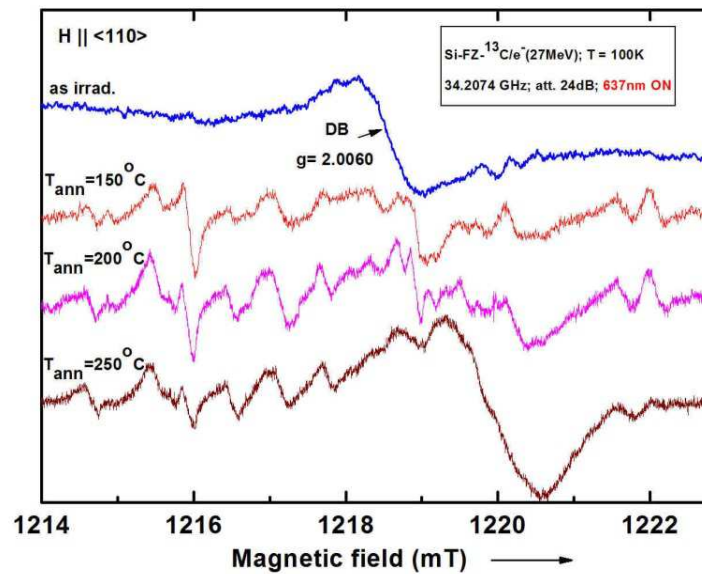
ESR spectra/lines from isotropic DB, GGA2 and P_o center.



The observed photoinduced (637nm) ESR signals, stable at $T < 150\text{K}$.

IIIB. Experimental results on e^- (27MeV) irradiated Si-FZ-13C samples.

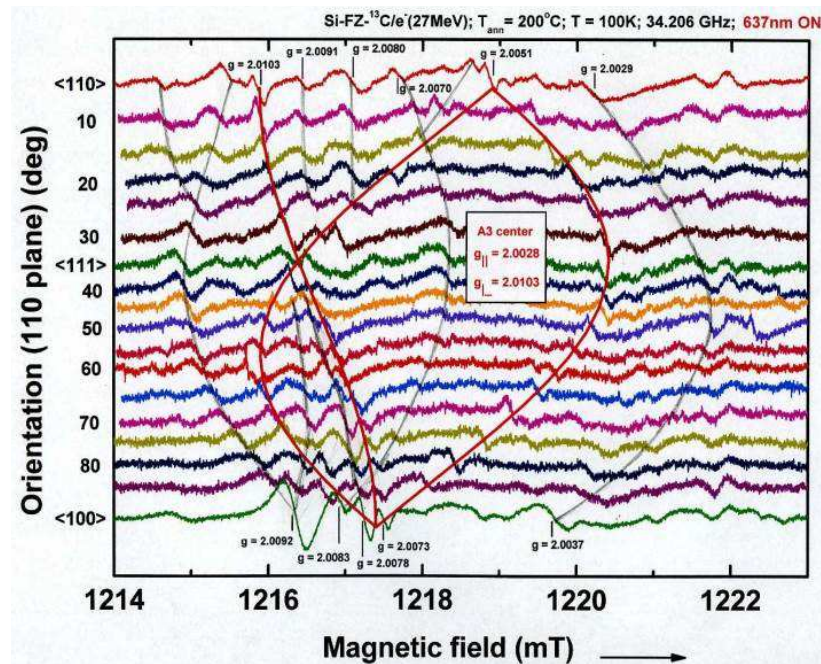
Thermal annealing produces changes in the photo induced ESR spectra/centers.



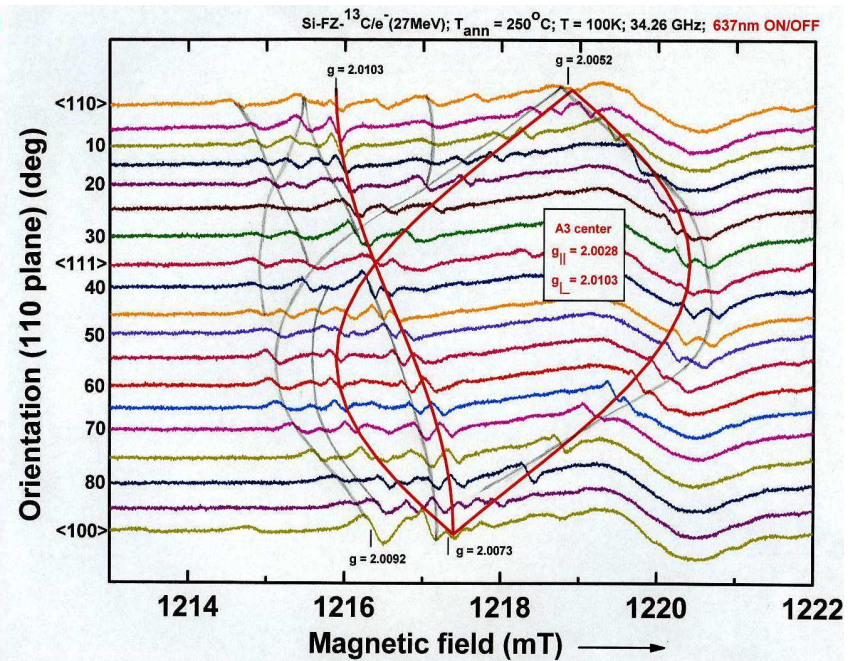
IPPDs in $T_{ann} = 150^\circ C$ sample.
Identified center (A3) – red lines.
Unidentified centers – black lines.

IIIB. Experimental results on e^- (27MeV) irradiated Si-FZ-13C samples.

Thermal annealing produced changes in the photo induced ESR spectra/centers.



$T_{\text{ann}}=200^\circ\text{C}$; $T_{\text{meas}}= 100\text{K}$
Absorption mode.



$T_{\text{ann}}=250^\circ\text{C}$; $T_{\text{meas}}= 100\text{K}$
Absorption mode.

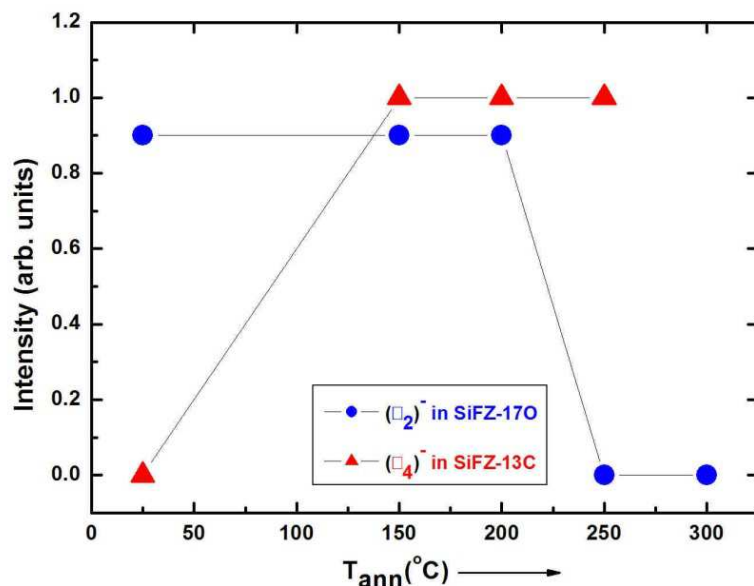
IV. Synthesis of results. Analysis of available data.

Center / symmetry	Host	g	T_{meas} (K)	Production	Annealing ($^{\circ}\text{C}$) / 637 nm bleaching
DB isotropic	SiFZ-17O SiFZ-13C	2.0060	300-10	As irradiated.	No 637nm effect.
GGA2 isotropic	SiFZ-13C	2.0028	< 50	As irradiated	$T_{\text{ann}} = 150\text{ }^{\circ}\text{C}$ No 637nm effect.
P_0 isotropic	SiFZ-13C	1.9999	100	As irradiated. Strong μW saturation	No 637nm effect.
idem	SiFZ-17O	1.9999	100	After $T_{\text{ann}}=150^{\circ}\text{C}$	No 637nm effect.
G7 / (\square_2)⁻ C3 <111>	SiFZ-17O	$g_{\parallel}=2.0115$ $g_{\perp}=2.0080$	<150	637nm photoinduced at $T < 150\text{K}$	$T_{\text{ann}} = 250\text{ }^{\circ}\text{C}$
A3 / (\square_4)⁻ C3 <111>	SiFZ-13C	$g_{\parallel}=2.0028$ $g_{\perp}=2.0103$	<150	637nm photoinduced ($T < 150\text{K}$) after $T_{\text{ann}}=150^{\circ}\text{C}$	$T_{\text{ann}} = 300\text{ }^{\circ}\text{C}$

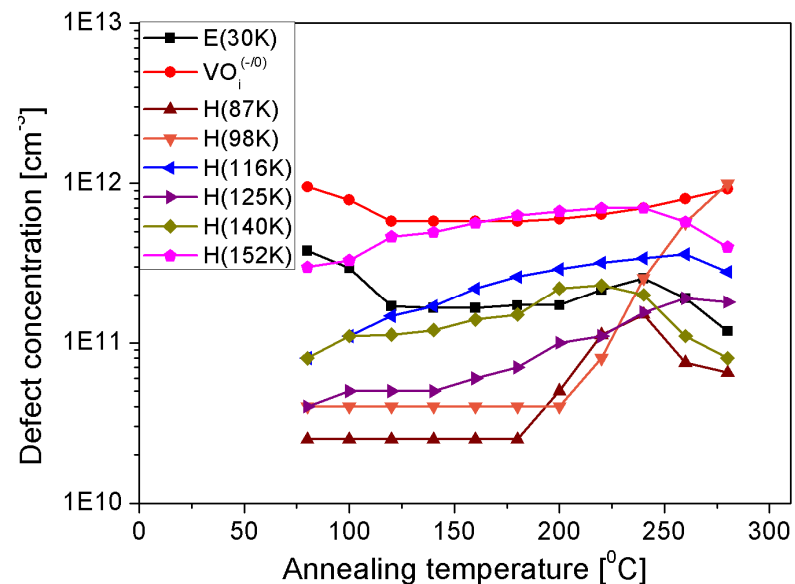
IV. Synthesis of results. Analysis of available data.

ESR spectra from other, still unidentified IPPDs, can be observed in the 637 nm optically excited samples at various annealing temperatures, in both type of investigated samples (SiFZ-17O and SiFZ-13C).

IV. Synthesis of results. Analysis of available data.



v(Si)-type defects conc. vs. T_{ann} in oxygen doped and depleted Si-FZ irradiated with 27MeV electrons



Results of isochronal annealing on DOFZ samples Si-FZ irradiated with 27MeV electrons

Remarks:

- In oxygen doped Si (DOFZ) the formation of divacancies (\square_2)[•] is a dominant process.
- Meanwhile the formation of tetravacancies (\square_4)[•] is slowed down, compared to samples with lower oxygen concentration (SiFZ-13C).
- The divacancies decay at $T_{ann} = 250$ °C.
- Correlation of defects conc. vs. T_{ann} from ESR and TSC measurements confirm that some of the H centers (in TSC studies) are vacancy based cluster defects.

V. Conclusions

- The standard (absorption) ESR measurements resulted in observation of a very limited number of IPPDs species.
- More IPPDs were observed by across the gap *in-situ* irradiation at $T < 150$ K, and in the saturated-dispersive mode ESR.
- Our investigations revealed a strong dependence of the production of IPPDs with the concentration of oxygen impurity, in both as-irradiated and further annealed samples.
- It is not yet clear the role (if any) played by the implanted carbon. Future measurements on ^{13}C implanted and annealed samples may offer an answer.

Determining the nature of many other IPPDs, revealed in this first stage of ESR measurements, remains our next main objective.

***The Research Center for Advanced ESR techniques (CetRESav)
form NIMP (<http://www.cetresav.infim.ro/>)***

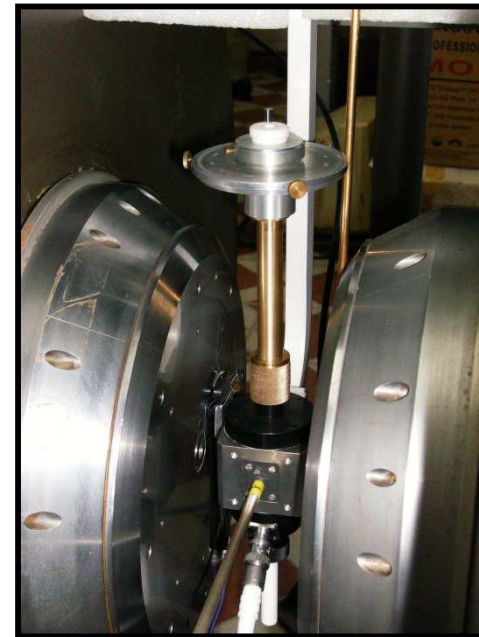
The research center for advanced ESR techniques from NIM conducts basic and applied researches in condensed matter physics, materials science and related scientific domains by advanced (CW and Pulse) multiresonance and multifrequency Electron Spin/Paramagnetic Resonance (ESR / EPR) methods and techniques.

- **X(9.5 GHz) and Q (34 GHz) CW ESR and ENDOR, EIE, triple resonance techniques.**
- **X - band pulse / Fourier Transform (FT) ESR, ENDOR, ELDOR, ESSEM, HYSCORE, ... techniques.**
- **Operation in the $3.8 < T < 300$ K temp. range**
- **Further developments : X- and Q – band ODMR**

CetRESav- CW X-band ESR spectrometer



The EMX-plus (Bruker) X-band spectrometer with Varian E12 magnet (NIMP - CetRESav)



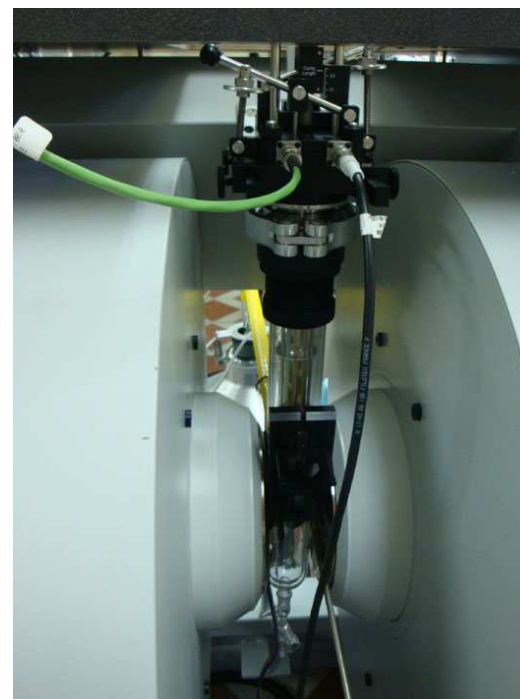
Goniometer mounted on the Premium X cylindrical cavity

Sensitivity: 2.5×10^9 spins/0.1mT; B range: 30 mT- 1.8 T; Stability (ν and B): $< 10^{-6}$; μ W freq. range: 9.3-9.9 GHz; μ W power range: $5 \times 10^{-1} - 2 \times 10^{-6}$ W; $3.8\text{K} < T < 500\text{K}$

CetRESav - CW Q-band ESR spectrometer



The Q-band CW ESR spectrometer ELEXSYS 500Q with E560 ENDOR unit



The Q-band ENDOR cavity in the cryostat for low temp. measurements

Sensitivity: 10^9 spins/0.1mT; B range: 30 mT- 1.8 T; Stability (f and B): $< 10^{-6}$;
uW frequency: 34 GHz; mW power range: 5×10^{-1} - 2×10^{-6} W; $3.8\text{K} < T < 300\text{K}$

CetRESav - FT/pulse X-band ESR spectrometer and the liquid He plant and recovery system



The X- band FT/pulse ESR spectrometer ELEXSYS 580
with E560 DICE ENDOR and E540 -400 pulse ELDOR



The LHeP18 (Cryomec) liquid He plant and
part of the He gas recovery system

Sensitivity (CW): 1.2×10^9 spins/0.1mT; B range: 30 mT- 1.45 T
Stability (f and B): $< 10^{-6}$; uW frequenc: 9.2-9.9 GHz;
max mW power: 1 kW; $3.8K < T < 300K$; Pulse resolution : 1 ns

CetRESav – Supporting equipment and software.

- **Single crystals and nanocrystals growth.**
- **Samples preparation (X-ray orientation, cutting, polishing, thermochemical treatments).**
- **Optical (UV-VIS-IR) absorption and emission spectroscopy.**
- **Software for ESR spectra analysis:**
 - **XSophe (Bruker)**
 - **WinEPR SimFonia (Bruker)**
 - **SIM (Prof. Hoegni Weihe, University of Copenhagen)**
 - **EasySpin (ETH-Zurich)**
 - **Origin TM**